Journal of Optoelectronics and Advanced Materials Vol. 7, No. 2, April 2005, p. 659 - 664

ON THE SYNTHESIS AND CHARACTERIZATION OF POLYCRYSTALLINE GaSb SUITABLE FOR THERMOPHOTOVOLTAIC (TPV) APPLICATIONS

A. Mitric*, Th. Duffar, A. Amariei[a], X. Chatzistavrou[a], E. Pavlidou[a], K. M. Paraskevopoulos[a], E. K. Polychroniadis[a]

EPM-CNRS, ENSHMG, BP695, 38402 St. Martin D'Hères, France
[a]Department of Physics, Aristotle University of Thessaloniki, 54124 Thessaloniki, Greece

For the growth of GaSb crystals, firstly the GaSb feed material must be prepared. An alternative method, based on magnetic induction phenomena, was used to synthesize GaSb feed materials. The advantage of this method is the mixing time, which is much shorter (3h) than for other methods (12h). In order to investigate the efficiency of the technique, GaSb feed material has been prepared and analyzed. This paper presents the results of this GaSb feed material characterization by different techniques. The stoichiometry and homogeneity of the samples were verified by Energy Dispersive Spectroscopy (EDS) and Transmission Electron Microscopy (TEM) and were found to be compositionally homogeneous having a stoichiometry very close to the nominal one. The optical behavior of the samples was studied using Fourier Transform Infrared (FTIR) Spectroscopy. Their optical parameters, calculated by fitting the FTIR reflectivity spectra, present a typical behavior, in accordance with the literature.

(Received August 18, 2004; accepted March 23, 2005)

Keywords: GaSb, Energy dispersive spectroscopy (EDS), Transmission Electron Microscopy (TEM)

1. Introduction

Thermophotovoltaic (TPV) cells are now one of the most attractive choice for producing electrical energy under specific conditions. The thermophotovoltaic (TPV) device use for converting radiation to energy the same principles as PV devices (solar cells), but TPV is expected to have a greater power density output due to its system geometries and the temperature of the radiator [1]. The idea of the TPV conversion appeared in the late 1950s but the real interest in this technology came later, in the beginning of 1990s, in conjunction with the introduction of the high quality low-bandgap semiconductors (III-V compounds and its alloys) used as converter material [1].

Among the III-V semiconductors, GaSb-based materials, ternary (by replacing Ga with In) or even quaternary alloys (by replacing Sb by As), are considered to be an efficient choice for TPV converters [2]. These materials are preferred because their bandgap covers a wide energy range and so suits well the emission wavelength band of low temperature (1000 – 1400 ˚C) selective TPV radiators.

Currently the binary GaSb is mostly used as substrate, for both epitaxial and diffused junction TPV devices, with reasonable efficiency [3]. Recent studies [4,5] show that TPV cells using polycrystalline GaSb wafers have almost the same high performance as in the case of the monocrystalline GaSb. Only for low voltage, the influence of grain boundaries can become visible, but this is not significant in the case of TPV cells, which work at high current densities. This can lower significantly the final cost of the TPV cell, as the wafer cost represents the predominant part of the final price.

* Corresponding author: adina@auth.gr

In this work a new method of synthesis for GaSb material is proposed. The characterization of the resulting materials was caried out, focusing on structural and optical characteristics. The structural characterization was performed by Transmission and Scanning Electron Microscopy (TEM,SEM) and additionally the stoichiometry and homogeneity of the GaSb samples was verified by Energy Dispersive Spectroscopy (EDS). Optical behaviour of samples was studied using Fourier Transform IR Spectroscopy (FTIR) and the characteristic optical parameters were calculated by fitting the FTIR reflectivity spectra.

2. Synthesis

An alternative technique based on electro-magnetic induction was developed for GaSb feed material elaboration**.**

The starting materials used for GaSb synthesis are 6N Ga and Sb. The synthesis is carried out in an evacuated and sealed silica ampoule 11 mm in diameter and 500 mm in length. Initially the ampoule is kept for 1h in HF in order to clean the vessel wall. Then the ampoule is rinsed in de-ionized water, pure ethanol and dried. Before the elaboration, Sb is etched to remove their oxide surface. Sb millimetric pieces are covered with pure HCl. H_2O_2 drops are slowly poured using a burette until the colour of the solution becomes green (the potential user should be cautious, as toxic Cl_2 fumes are produced). Then the Sb is rinsed 3 times in pure HCl, then de-ionized water until the pH becomes neutral, and finally in pure ethanol. Ga is used as received, by pouring fresh drops in the silica tube. In a first phase the clean Ga drops are introduced into the quartz ampoule, and then heated under vacuum for degasification. Then the ampoule is filled with the appropriate amount of Sb in order to get stoichiometry and sealed under dynamic vacuum. The ration of Ga atoms to Sb atoms is 1:1 corresponding to a ratio by weight of 1:1.75.

The device used for the synthesis is an induction coil surrounding the silica tube which is held in a ceramic drilled cylinder (Fig. 1). A high frequency alternating current (20 kHz) is applied to the coil, generating an alternating magnetic field. When the silica ampoule filled with Ga and Sb is located in the coil, electro-magnetic currents (Foucault currents) are induced, heating and melting the materials by Joule effect. The temperature is measured and controlled by 2 thermocouples. The induction heating power supply is controlled in order to obtain 800-900 °C on the crucible external surface. The currents interact with the electromagnetic field, generating electromagnetic forces (Lorentz forces). These forces are responsible for the intimate liquid material mixing and consequently for the acceleration of the element reaction. After waiting 3 hours, the obtained material is solidified by pulling slowly the crucible out of the coil with a rate of 1mm/min.

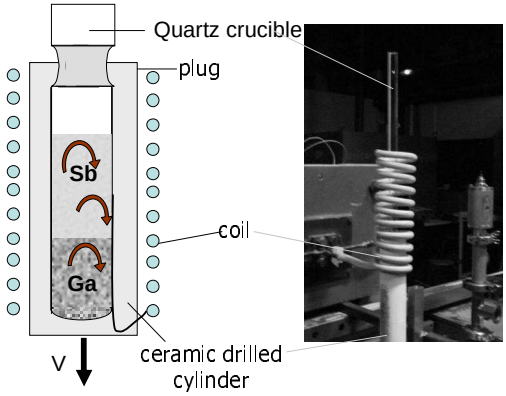

Fig. 1. Experimental device.

In order to verify the reproducibility of the method, two growth experiments were carried out (named 1 and 2) under the same growth conditions. From the two ingots two slices were cut, one

from the bottom (named A) and one from the top part (named B), vertical to the growth direction. In order to improve the quality surface the samples were polished with silicon carbide (the SiC- 240, 600, 800, 1200, 2400) and diamond paste (6 μm, 3 μm). So the characterization was carried out on four samples in order to compare not only the two ingots but also the homogeneity along the axis of the ingot.

3. Homogeneity

EDS analysis gives directly the elemental percentage, from which the stoichiometry of each compound is calculated. The analysis was performed in JSM 840A SEM, equipped with an Oxford ISIS EDS analyzer. EDS analysis is sensitive to the surface orientation with respect to the electron beam as well as the crystallographic orientation of the grains. That is why, considering the polycrystalline character of all samples, the accuracy of the final result is limited up to ± 2 at %. The accuracy was partially improved by a good polishing of the surface. The EDS analysis was performed in 15 points of each sample in radial direction and a mean value of these was considered, in order to have a better picture of the grown material. The EDS results, for the GaSb samples are shown in Table 1

Table 1. EDS analysis of GaSb samples.

	Ga (at%)	Sb (at%)
1 - A	47.5	51.4
1 - B	45.6	54.4
2 - A	48.2	51.8
2 - B	47.9	52.1

As shown by the results, the deviations from point to point in the same section are within the experimental errors. This means that there is a radial homogeneity. However the main finding is that there is an excess of Sb, contrary to the Ga content, in the whole ingot.

4. Structural properties

The structural properties of the grown material were studied by a conventional TEM (JEM 100C) operating at 100 keV. Having in mind that the observable area in TEM is very limited, several specimens were prepared from all four samples in order to have a more complete view of the material, but mainly to detect any differences, if any, existing between the two ingots, as well as the two parts that are examined from the same ingot. A possible preferential crystallographic orientation in respect to the growth direction was also examined.

TEM study shows similar characteristics for all samples including a big variety of structural defects i.e. low angle boundaries, subgrain boundaries, and, of course, dislocations. Fig. 2 shows a mixed type low angle boundary, where there are two sets of dislocations with different equidistance.

Also Fig. 3 shows a characteristic twin, which is a rotational one of [111] type. Finally it is concluded that there is no preferential orientation between the grains and the dislocations are not homogeneously distributed in the whole samples. The only detectable difference is between the top part and the bottom of the ingots. Although all the observed samples are stressed the upper parts of the ingots are more stressed than the bottom parts. The last ones present fewer cracks during thinning.

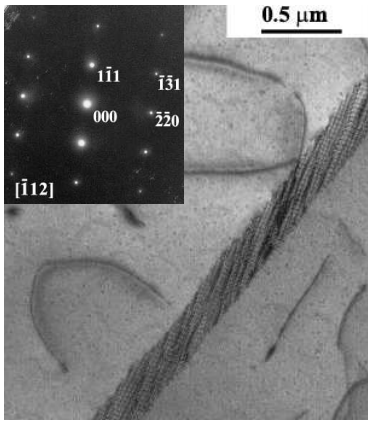

Fig. 2. TEM image showing a mixed low angle boundary.

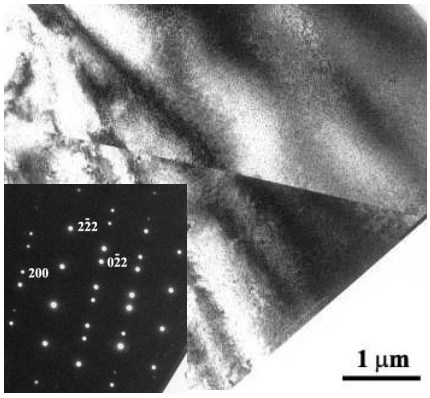

Fig. 3. TEM image showing a [111] rotational twin.

5. FTIR characterization

Optical properties of the studied compounds were determined from their room temperature reflectivity spectra. The spectra were taken with the spectrometer Bruker IFS 113v working under vacuum, in spectral region 1000 – 50 cm^{-1}. The resolution of the measurements was 2 cm^{-1} and each spectrum was obtained by recording 64 consecutive scans.

Fig. 4 (a, b) presents characteristic reflectivity spectra of samples grown with the new proposed method, from bottom and top of the ingot. In these spectra, one reflectance band is clearly evident. Reststrahlen bands in all samples are around 226 cm^{-1} (ωTO), while at lower wavenumbers the free carrier plasma edge is identified, close to the high reflection tail due to the increased number of carriers, although the ingot is undoped, consequently being continuously p-type [6].

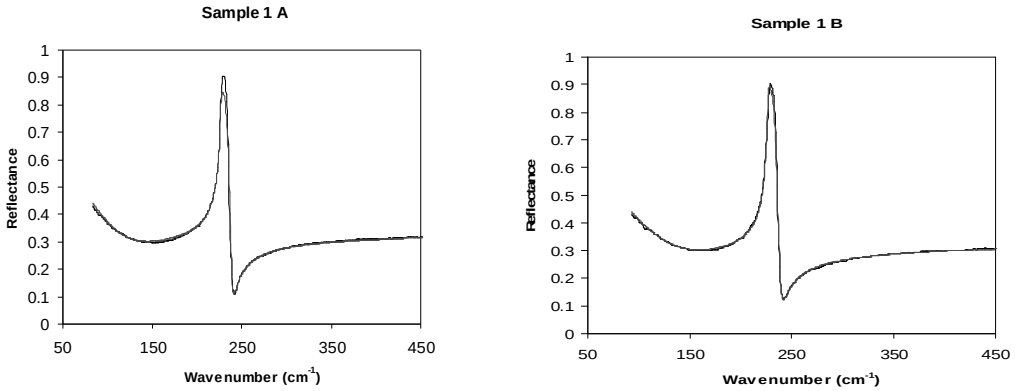

Fig. 4(a, b). Reflectivity spectra of the samples 1A and 1B.

The reflectivity spectra were first analyzed using Kramers-Kronig (K-K) analysis. The K-K dispersion relations allow the calculation theoretically of the dielectric constants of a solid starting from its known reflectivity curve. TO-phonon frequencies ω_{TO} were estimated from the positions of the relative maxima in the imaginary part of the dielectric constant ε_2, and LO-phonon frequencies ω_{LO} were estimated from the positions of the maxima in the energy loss term Im(-1/ε). The phonon characteristics as estimated from the K-K analysis were then used as starting values in a Lorentzian oscillator formalism to synthesize a reflectivity spectrum. Analytically, using such estimates for the

values of frequency, strength, and line width, fits to reflectivity were carried out using an expansion of the complex dielectric function $\varepsilon(\omega)$ in the form of a sum of classical-oscillator terms:

$$\varepsilon(\omega) = (n - ik)^2 = \varepsilon_\infty + \frac{\Delta\varepsilon \cdot {\omega_{TO}}^2}{{\omega_{TO}}^2 - \omega^2 - i\omega\gamma_{TO}} - \frac{\varepsilon_\infty {\omega_P}^2}{\omega(\omega + i\gamma_P)} \tag{1}$$

where n and k are the refractive and absorption indices respectively, ε_∞ is the high-frequency dielectric constant, $\Delta\varepsilon$ the oscillator strength, ω_P the plasmon frequency and γ_{TO}, γ_P are the phonon and plasmon damping constants respectively [6].

By varying the parameters of each oscillator to obtain the best fit of theory to the reflectivity data, we obtain more accurate values of the TO-mode parameters, ω_{TO}, $\Delta\varepsilon$ and γ_{TO} than could be estimated from the original K-K analysis.

The studied samples presented a relatively high carrier concentration so that the plasmon frequencies were in the vicinity of the lowest lattice frequency of interest. For this reason the analysis of the reflectivity spectra was performed taking into account the contribution of plasmon mode as the plasmon phonon coupling is efficient and affects the spectrum on the high energy side of the reststrahlen band [7].

From the optical reflectivity measurements the optical mobility and conductivity can be calculated with the use of the formulas:

$\mu = \frac{9328}{m^* \cdot \gamma_p}$ [cm^2/V]	$\sigma = \frac{2\pi \cdot \varepsilon_\infty \cdot {\omega_p}^2}{377 \cdot \gamma_p}$ [Ohm^{-1}·cm^{-1}]

Table 2 presents the oscillator parameters for each of the studied places in the ingots. The phonon frequencies as obtained from K-K analysis and oscillator fitting are in good agreement with each other.

Table 2. Oscillator parameters for each composition.

	ω_{TO} (cm^{-1})	γ_{TO} (cm^{-1})	ω_{LO} (cm^{-1})	$\Delta\varepsilon$	ε_∞	ω_p (cm^{-1})	γ_p (cm^{-1})
1 A	226.4	2.15	235.9	1.20	14.00	123.8	116.11
1 B	226.6	1.26	235.8	1.12	13.63	140.8	135.52
2 A	226.3	2.26	235.8	1.24	14.46	119.1	109.00
2 B	226.6	0.89	235.7	1.16	14.04	129.2	184.13

From the results of the spectroscopic analysis included in the table it can easily understood that the ingot can be considered as typical GaSb presenting stability in the phonon frequencies (ωTO, ωLO). Examining in more details the results of the same ingot, we follow a remarkable difference in the plasmon parameters, presenting the same tendency in the studied samples. Analytically, the plasmon frequency is increased from the bottom to the end of the ingot and the damping constant of the mode is also decreased. Connecting these findings with the other parameters of the material we can say that the number of carriers n, in the same ingot, is higher (for sample 1A $n = 5.51 \times 10^{17}$ and $n = 6.95 \times 10^{17}$ for 1B) at the end point suggesting an increased number of structural defects, as it is concluded and from the other observations. On the contrary, the value of the optical mobility is decreased going (for the ingot A) from the value of μ= 349 cm^{2}V^{-1}s^{-1}

at the beginning, to the value $\mu = 299$ $cm^2V^{-1}s^{-1}$ at the end and this can be related to the presence of cracks, discussed above.

6. Conclusions

A new method for the synthesis of polycrystalline GaSb feed material is proposed based on electro-magnetic induction. EDS analysis reveals an excess of Sb, in the whole ingot. Microstructural characterization concludes that there is no preferential orientation between the grains, and the dislocations (among the other structural defects) are not homogeneously distributed in the samples. Additionally, it was deduced that the upper parts of the ingots are more stressed that the bottom parts.

The samples present typical GaSb behaviour as it concerns their phonon characteristics, confirming the chemical type of the grown material. From the other side, the number of carriers is rather higher than in samples studied in the literature and this characteristic is related to the increased Sb percentage. In the same ingot, the concentration of the carriers increases from the bottom to the end by about 20% and this can be attributed to the increased number of structural defects, while the optical mobility is decreased by 20-30% going from the beginning to the end of the ingot, this being related to the presence of the cracks.

Acknowledgement

This work was supported by the European Project "TPV cells based on GaSb", Contract no: HRRN-CT 2001-00199

References

[1] T. J. Coutts 1999 Renew. Sustainable Energy Rev. **3**, 77-184.
[2] A. W. Bett, O. V. Sulima, Semicond. Sci. Technol. **18**, S184 – S190 (2003).
[3] R. Beckert, L. Broman, K. Jarefors, J. Marks, K. Bücher, Measurement comparison of InGaAs- and GaSb-based (thermo-) photovoltaic cells with two different methods, Second World Conference on PV Solar Energy Conversion 30 (1998).
[4] L. M. Frass, R. Ballantyne, S. Hui, S. Ye, S. Gregory, J. Keyes, J. Avery, D. Lamson, B. Daniels, 1998 4th NREL Conf. on the Thermophotovoltaic Generation of Electricity (AIP Conf. Ser.) vol. 460, ed T. J. Coutts, C. S. Allman and J. Benner, 1998, pp. 480-7.
[5] O. V. Sulima, A. W. Bett, P. S. Dutta, H. Eshani, J. Gutman, 2000 Proc 16th European Photovoltaic Solar Energy Conf. and Exhibition (Glasgow) pp 169-72.
[6] R. Ferrini, G. Guizzetti, M. Patrini, A. Bosacchi, S. Franchi, R. Magnanini, Solid State Communications **104**, 747 (1997).
[7] C. J. Pickering, Phys. C: Solid St. Phys. **13**, 2959 (1980).